

QED corrections to the g factor of Li- and B-like ionsH. Cakir ^{1,*}, V. A. Yerokhin ^{1,2}, N. S. Oreshkina ¹, B. Sikora,¹ I. I. Tupitsyn,³ C. H. Keitel ¹ and Z. Harman¹¹Max Planck Institute for Nuclear Physics, Saupfercheckweg 1, 69117 Heidelberg, Germany²Peter the Great St. Petersburg Polytechnic University, 195251 St. Petersburg, Russia³Department of Physics, St. Petersburg State University, Universitetskaya 7/9, 199034 St. Petersburg, Russia

(Received 13 January 2020; accepted 24 March 2020; published 17 June 2020)

QED corrections to the g factor of Li-like and B-like ions in a wide range of nuclear charges are presented. Many-electron contributions as well as radiative effects on the one-loop level are calculated. Contributions resulting from the interelectronic interaction, the self-energy effect, and most of the terms of the vacuum-polarization effect are evaluated to all orders in the nuclear coupling strength $Z\alpha$. Uncertainties resulting from nuclear size effects, numerical computations, and uncalculated effects are discussed.

DOI: [10.1103/PhysRevA.101.062513](https://doi.org/10.1103/PhysRevA.101.062513)**I. INTRODUCTION**

Precision studies of g factors of highly charged ions (HCI) provide a unique possibility for testing fundamental theories. Penning-trap experiments employing the continuous Stern-Gerlach effect achieve high precision nowadays, and are advancing towards heavy ions, in which the effects of quantum electrodynamics (QED) are most relevant. The g factor of hydrogenlike silicon ($Z = 14$) has been determined with a 5×10^{-10} fractional uncertainty [1,2], allowing one to scrutinize the bound-state QED theory (see, e.g., [3–11]). Recently, the evaluation of two-loop terms of order $(Z\alpha)^5$ (with Z being the atomic number and α the fine-structure constant) has been finalized [12] (see also [13]), increasing the theoretical accuracy especially in the low- Z regime. First milestones have been reached in the calculation of two-loop corrections for nonperturbative Coulomb fields, i.e., for larger values of $Z\alpha$ [14,15].

The high accuracy which can be achieved on the experimental as well as theoretical side also enables the determination of fundamental physical constants such as the electron mass [16–18]. However, QED tests as well as the extraction of fundamental constants may be limited by nuclear effects [11,19–21]. Since the nuclear parameters entering the nuclear corrections are not always sufficiently well known, these corrections may be associated with large uncertainties, and thus set a natural limit to the accuracy of the theoretical g factor.

The extension of experiments to the heaviest ions, including Pb^{81+} and U^{91+} , is expected in the forthcoming years by

the use of the ALPHATRAP Penning-trap setup [22] and the HITRAP facility [23,24]. Measurements with these systems are anticipated to provide an alternative determination of the value of α [25–27]. In Ref. [25], a specific (or weighted) difference of the g factors of heavy H- and B-like ions with the same nuclear species was put forward. It was demonstrated that the theoretical uncertainty of the nuclear finite size effects in this difference can be suppressed down to 4×10^{-10} for very heavy ions such as Pb, which was several times smaller than the theoretical uncertainty of the g factor due to α at that time. In Refs. [26,27] a specific difference of the g factors of low- Z H- and Li-like ions was proposed, for which an even stronger suppression of nuclear effects and their uncertainties can be achieved, leading to an accuracy competitive with the current value of α . A calculation of the nuclear polarization effect extended to Li- and B-like ions showed that these terms can also be largely suppressed in a specific difference of the g factors for two different charge states of the same element [28].

Motivated by these prospects, in the current paper, we calculate the ground-state g factor of Li- and B-like HCI. Our results for Li-like ions confirm previous calculations. We extend the computations for B-like Ar^{13+} presented in [29] for a range of elements across the periodic table, and describe them in detail in the current paper. The one-electron self-energy term is calculated with an improved numerical accuracy. The vacuum polarization screening diagrams are evaluated, and self-energy screening is estimated using effective screening potentials. Electron correlation effects are taken into account by exact QED methods up to order $1/Z$, and higher-order terms are extracted from large-scale relativistic configuration interaction calculations.

This paper is organized as follows. In Sec. II, we discuss relativistic and electron-correlation contributions to the bound-electron g factor. In Secs. III and IV, we describe our computations of the self-energy and vacuum-polarization contributions, respectively. In Sec. VI, we tabulate and discuss our computations of the contributions to the bound-electron g factor and provide concluding remarks. We use relativistic units ($\hbar = c = m_e = 1$) and the Heaviside charge unit ($\alpha = e^2/(4\pi)$, $e < 0$).

*This article comprises parts of the Ph.D. thesis work of H.C., submitted to Heidelberg University, Germany; halil.cakir@mpi-hd.mpg.de

Published by the American Physical Society under the terms of the Creative Commons Attribution 4.0 International license. Further distribution of this work must maintain attribution to the author(s) and the published article's title, journal citation, and DOI. Open access publication funded by the Max Planck Society.

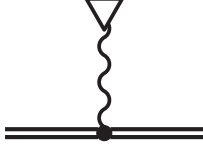


FIG. 1. The Feynman diagram representing the leading contribution to the bound-electron g factor. Double lines represent electrons in the electric field of the nucleus and a wavy line with a triangle represents an interaction with the external magnetic field.

II. RELATIVISTIC g FACTOR

The Zeeman shift linear in the magnetic field of an energy level of an atom with a spinless nucleus is parametrized in terms of the g factor of the atom by the equation

$$\Delta E = g \mu_B \langle \mathbf{J} \cdot \mathbf{B} \rangle, \quad (1)$$

where ΔE is the energy shift, \mathbf{J} is the operator of the total angular momentum, \mathbf{B} is the external magnetic field, $\mu_B = |e|/2$ denotes the Bohr magneton, and g is the g factor. The g factor is determined by computing the Zeeman energy splitting and solving Eq. (1) for g .

The relativistic interaction of an electron with the homogeneous external magnetic field is given by

$$V_{\text{mag}}(\mathbf{r}) = -e\boldsymbol{\alpha} \cdot \mathbf{A}(\mathbf{r}), \quad (2)$$

where $\boldsymbol{\alpha}$ denotes the vector of Dirac matrices and \mathbf{A} is the vector potential $\mathbf{A}(\mathbf{r}) = (\mathbf{B} \times \mathbf{r})/2$. Assuming that the magnetic field is directed along the z axis, V_{mag} reduces to

$$V_{\text{mag}}(\mathbf{r}) = \frac{|e|B_z}{2} (\mathbf{r} \times \boldsymbol{\alpha})_z. \quad (3)$$

An *ab initio* QED theory of the g factor of an atom can be formulated, e.g., within the two-time Green's function formalism [30]. Within this formalism, the Zeeman energy splitting is calculated.

A. Dirac value and nuclear size contribution

The leading contribution to the g factor of an alkali-like atom arises through the interaction of the valence electron with the external magnetic field. The corresponding Feynman diagram is depicted in Fig. 1. Within the approximation of noninteracting electrons, contributions resulting from the interaction of the closed-shell core electrons with the external magnetic field cancel in the final sum, since electrons with opposite spin projections induce contributions of the same magnitude but of opposite sign. Therefore, only the contribution of the valence electron remains. For this reason, the g factor of the whole alkali-like atom is often termed as the bound-electron g factor (assuming that of the valence electron).

The leading (Dirac) contribution to the bound-electron g factor of an alkali-like atom with the valence state characterized by the quantum numbers n and κ is

$$g_D = \frac{2\kappa}{j(j+1)} \int_0^\infty dr r G_{n\kappa}(r) F_{n\kappa}(r), \quad (4)$$

where $j = |\kappa| - 1/2$ is the total angular momentum quantum number, and the functions $G_{n\kappa}$ and $F_{n\kappa}$ are the radial

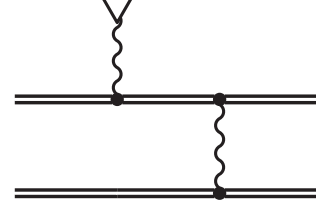


FIG. 2. A typical Feynman diagram representing the one-photon interelectronic-interaction contribution to the bound-electron g factor. Only diagrams where one of the electrons is the valence electron and the other one a core electron contribute.

components of the electronic wave function

$$\psi_{n\kappa m}(\mathbf{r}) = \frac{1}{r} \begin{pmatrix} G_{n\kappa}(r) \Omega_{\kappa m}(\mathbf{n}) \\ i F_{n\kappa}(r) \Omega_{-\kappa m}(\mathbf{n}) \end{pmatrix}, \quad (5)$$

where $\Omega_{\kappa m}(\mathbf{n})$ are spherical spinors.

For a pointlike (pnt) nucleus, the integral in Eq. (4) can be evaluated analytically, with the result [31,32]

$$g_D(\text{pnt}) = \frac{\kappa}{2j(j+1)} (2\kappa \varepsilon_{n\kappa} - 1), \quad (6)$$

where $\varepsilon_{n\kappa}$ is the Dirac energy of the reference state. In particular, for the $2s$ and $2p_{1/2}$ states relevant for this work, they are

$$\varepsilon_{2s} = \varepsilon_{2p_{1/2}} = \sqrt{\frac{1+\gamma}{2}}, \quad (7)$$

where $\gamma = \sqrt{1 - (Z\alpha)^2}$.

The nuclear size correction to the point-nucleus Dirac value is determined as the difference of Eq. (4) evaluated numerically for an extended nuclear charge distribution and the point-nucleus result of Eq. (6). We use the homogeneously charged sphere as the model for an extended nucleus with the rms radii taken from Ref. [33]. We estimate the dependence on the model by also using the two-parameter Fermi distribution and find it to be insignificant compared to the uncertainties associated with other contributions.

B. First-order interelectronic interaction

Interactions among the electrons in a multielectron ion result in a contribution to the bound-electron g factor. These interactions can be classified according to the number of exchanged photons and the associated perturbation parameter is $1/Z$.

We compute the leading one-photon exchange contribution, which corresponds to the first-order perturbation correction in the parameter $1/Z$. A typical contributing diagram is depicted in Fig. 2. As seen in the figure, the computation of the one-photon exchange contribution reduces the many-electron problem to a two-electron one, where one of the core electrons interacts with the valence electron in addition to the interaction with the external magnetic field. Analogous contributions from the exchange between core electrons vanish, again, identically after summing over the spin projections of the closed-shell core states.

The one-photon exchange contribution to the Zeeman shift of an energy level can be expressed as the sum of an

irreducible and a *reducible* part; the corresponding formulas were derived in Ref. [34]. The irreducible part arises from the first-order perturbative correction to the bound-electron wave function,

$$|\delta a\rangle = \sum_n^{\varepsilon_n \neq \varepsilon_a} \frac{\langle n | V_{\text{mag}} | a \rangle}{\varepsilon_a - \varepsilon_n} |n\rangle, \quad (8)$$

where a is either a core-electron state c or a valence-electron state v and the summation label n runs over the whole electronic spectrum including all bound states except the reference state a . The irreducible contribution is then given by

$$\begin{aligned} \Delta E_{\text{int,irr}}^{(1)} = & 2 \sum_c (\langle vc | I(0) | \delta vc \rangle - \langle cv | I(\Delta_{vc}) | \delta vc \rangle \\ & + \langle vc | I(0) | v \delta c \rangle - \langle cv | I(\Delta_{vc}) | v \delta c \rangle), \end{aligned} \quad (9)$$

where the summation is carried out over all core states, $\Delta_{vc} = \varepsilon_v - \varepsilon_c$ is the difference between the Dirac energy levels of the valence and core electrons, I is the operator of the electron-electron interaction,

$$I(\omega, \mathbf{r}_1, \mathbf{r}_2) = e^2 \alpha_1^\mu \alpha_2^\nu D_{\mu\nu}(\omega, \mathbf{r}_{12}), \quad (10)$$

$\alpha^\mu = (1, \boldsymbol{\alpha})$ are the Dirac matrices, $D_{\mu\nu}$ is the photon propagator, and $\mathbf{r}_{12} = \mathbf{r}_1 - \mathbf{r}_2$.

The reducible contribution arises from first-order perturbations of the energies of the core and valence electrons by the magnetic interaction, $\varepsilon_a \mapsto \varepsilon_a + \langle a | V_{\text{mag}} | a \rangle$. It is given by

$$\Delta E_{\text{int,red}}^{(1)} = \sum_c \langle cv | I'(\Delta_{vc}) | vc \rangle (\langle c | V_{\text{mag}} | c \rangle - \langle v | V_{\text{mag}} | v \rangle), \quad (11)$$

where the prime on $I'(\omega)$ denotes the derivative with respect to ω .

For the numerical computation of the one-photon exchange correction we solve the radial Dirac equation using basis sets constructed from B splines within the dual kinetic balance approach [35,36]. This approach is particularly suited for the computation of spectral sums as in Eq. (8). In our numerical treatment of the radial Dirac equation we take the nuclear size into account by using a homogeneously charged sphere as a nucleus with rms radii taken from Ref. [33]. The contributions are calculated using the Feynman and Coulomb gauges in order to estimate the numerical uncertainty. We present our result in Table I. Our calculations of the one-photon exchange correction reproduce previous results obtained in Ref. [34] for Li-like ions and Refs. [37,38] for B-like ions.

C. Higher-order interelectronic interaction

Electron correlation effects beyond the first-order approximation in $1/Z$, described in the previous section, were taken into account by means of a relativistic configuration interaction Dirac-Fock-Sturm (CI-DFS) approach, employing Dirac-Hartree-Fock orbitals for the occupied states and relativistic Sturmian orbitals for the virtual electronic states as in Ref. [39]. The contribution of the negative-energy part of the Dirac spectrum, which was found to be relevant in the case of g factors of Li-like ions in Ref. [40], is also significant in the case of B-like ions, and the corresponding states were also described with Sturmian orbitals.

TABLE I. First-order interelectronic-interaction contribution to the bound-electron g factor of the ground state of Li- and B-like ions. The uncertainties account for uncertainties in the nuclear rms radii and numerical errors.

Z	Electron correlation, $(1/Z)^4$	
	Li-like	B-like
18	0.000 414 450 489 (3)	0.000 657 531 117 (1)
20	0.000 461 147 896 (3)	0.000 731 996 913 (1)
24	0.000 555 185 23 (1)	0.000 882 350 695 (5)
32	0.000 746 458 66 (1)	0.001 190 274 990 (5)
54	0.001 306 216 8 (4)	0.002 118 178 3 (3)
82	0.002 148 290 (1)	0.003 654 888 (2)
92	0.002 509 828 (7)	0.004 393 71 (1)

The one-photon exchange correction results in the Breit approximation were used to monitor the convergence of the CI calculations when systematically extending the Sturmian basis set in the latter. The configurations obtained by single, double, and triple excitations of the ground state were included in the calculation. The one-electron functions up to $n = 10$ and $\ell = 5$ were included, leading to the total number of over 100 000 configurations. The theoretical uncertainty was estimated as twice the difference of the results using the largest and the second-largest Sturmian basis sets.

III. SELF-ENERGY

A. One-electron self-energy

To the zeroth order in $1/Z$, we can ignore the presence of the core electrons and evaluate the self-energy (SE) correction assuming the reference state being the hydrogenic Dirac state of the valence electron v .

The SE contribution to the energy shift of the hydrogenic state v in the presence of a perturbing potential V_{mag} is graphically represented by the Feynman diagrams shown in Fig. 3. The general expression for the SE correction can be conveniently split into three parts [30],

$$\Delta E_{\text{SE}} = \Delta E_{\text{SE,irr}} + \Delta E_{\text{SE,red}} + \Delta E_{\text{SE,ver}}, \quad (12)$$

which are referred to as the *irreducible*, the *reducible*, and the *vertex* contribution, respectively.

The irreducible contribution is induced by a part of the diagrams in Figs. 3(a) and 3(b) that can be expressed in terms of the first-order perturbation of the reference-state wave function by V_{mag} given in Eq. (8),

$$\Delta E_{\text{SE,irr}} = 2 \langle v | \gamma^0 \tilde{\Sigma}(\varepsilon_v) | \delta v \rangle, \quad (13)$$

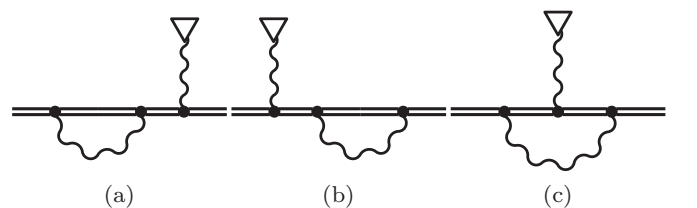


FIG. 3. Feynman diagrams representing the self-energy contribution to the bound-electron g factor.

where $\tilde{\Sigma} = \Sigma - \delta m$, δm is the one-loop mass counterterm, and Σ is the one-loop SE operator,

$$\Sigma(\varepsilon, \mathbf{r}_1, \mathbf{r}_2) = 2i\alpha\gamma^0 \int_{C_F} d\omega \alpha_\mu G(\varepsilon - \omega, \mathbf{r}_1, \mathbf{r}_2) \alpha_\nu D^{\mu\nu}(\omega, \mathbf{r}_{12}). \quad (14)$$

Here, G denotes the Dirac Coulomb Green's function $G(\varepsilon) = [\varepsilon - \mathcal{H}(1 - i0^+)]^{-1}$, \mathcal{H} is the Dirac Coulomb Hamiltonian, and C_F denotes the standard Feynman integration contour.

The reducible contribution is induced by a part of the diagrams in Figs. 3(a) and 3(b) that can be expressed in terms of the first-order perturbation of the reference-state energy. It reads

$$\Delta E_{\text{SE,red}} = \langle v | \gamma^0 \Sigma'(\varepsilon_v) | v \rangle \langle v | V_{\text{mag}} | v \rangle, \quad (15)$$

where the prime on $\Sigma'(\varepsilon)$ denotes the derivative with respect to ε .

Finally, the vertex contribution is induced by the diagram in Fig. 3(c). It can be expressed as

$$\Delta E_{\text{SE,ver}} = \frac{i}{2\pi} \times \int_{-\infty}^{+\infty} d\omega \sum_{n_1, n_2} \frac{\langle n_1 | V_{\text{mag}} | n_2 \rangle \langle v n_2 | I(\omega) | n_1 v \rangle}{(\varepsilon_v - \omega - u\varepsilon_{n_1})(\varepsilon_v - \omega - u\varepsilon_{n_2})}, \quad (16)$$

where $u = 1 - i0^+$ and the summations over n_1 and n_2 involve both the positive-energy discrete and continuous spectra and the negative-energy continuous spectrum.

Calculations of the SE correction to the g factor for the hydrogenic states are rather complicated but well established by now. For the point-nucleus case, the most accurate computations were performed in Refs. [8,41,42]. The finite nuclear size correction was computed in Ref. [43]. In the present work, we employ the numerical approach developed in those studies and extend the previous calculations to the case of the $2p_{1/2}$ reference state (required for B-like ions) and nuclear charges $Z > 12$, which has not been reported in the literature.

B. Screened self-energy

The interaction of the valence electron with the core electrons modifies the SE effect and the resulting energy shift is known as the *screened* SE correction. It is suppressed by a small parameter $1/Z$ as compared to the leading SE contribution.

A rigorous QED calculation of the screened SE correction to the g factor has been performed in Refs. [44,45] for four Li-like ions (with $Z = 14, 20, 82$, and 92). This was a very difficult calculation, which has not been so far extended to any other ion. Two less sophisticated methods exist in the literature for an approximate treatment of the screening of the SE corrections. One method, used in Ref. [46], evaluates the one-electron SE correction in the presence of an additional screening potential resulting from the interaction with the core electrons. Another method [47] describes the electron self-energy by the anomalous magnetic moment, which yields results complete to order $(Z\alpha)^2$ for s states. In the following, we address these two methods in turn.

1. Screening-potential approximation

Within the screening-potential approximation, we consider the electron in the combined field of the nucleus and an additional screening potential V_{scr} that partly accounts for the interaction of the valence electron with the core electrons. The simplest choice of V_{scr} is the core-Hartree (CH) potential defined as

$$V_{\text{CH}}(r) = 4\pi\alpha \int_0^\infty dr' r'^2 \frac{\rho_{\text{core}}(r')}{r_>}, \quad (17)$$

where $r_>$ is the larger one of r and r' , and ρ_{core} denotes the combined radial charge density of the core electrons in units of the elementary charge. In the present work we use also two other choices of the screening potential, namely, the Kohn-Sham (KS) potential and the local Dirac-Fock (LDF) potential, which are described in detail in Ref. [48]. All screening potentials are constructed with the Dirac-Fock wave functions.

Within the screening-potential approximation, the screened SE effect is obtained by evaluating the SE correction according to Eqs. (12)–(16) for the valence electron in the combined field of the nucleus and V_{scr} and subtracting the SE correction in the nuclear field. In this calculation, we generalized the numerical approach of Ref. [8] for computing the SE correction to the g factor to the case of an arbitrary binding potential. We used the Green's-function technique, with the Green's function of the Dirac equation in a general (asymptotically Coulomb) potential being computed by the method described in the Appendix of Ref. [49].

2. Anomalous magnetic moment approximation

The second method for the approximate treatment of the SE correction is based on the nonrelativistic expansion. As demonstrated in Ref. [50], to leading order in $Z\alpha$, which is here $\propto (Z\alpha)^2$, the SE correction to the bound-electron g factor of an s state is induced by the interaction of the anomalous magnetic moment (amm) of the electron with the electric and magnetic field in the atom. The interaction can be represented by the following effective Hamiltonian:

$$H_{\text{amm}} = \sum_j [H_1(j) + H_2(j)] + \sum_{j \neq k} H_3(j, k), \quad (18)$$

where j and k numerate electrons and

$$H_1(j) = a_e \mu_B \beta_j \mathbf{B} \cdot \boldsymbol{\Sigma}_j, \quad (19)$$

$$H_2(j) = a_e \frac{Z\alpha}{2} (-i) \beta_j \frac{\boldsymbol{\alpha}_j \cdot \mathbf{r}_j}{r_j^3}, \quad (20)$$

$$H_3(j, k) = a_e \frac{\alpha}{2} \left(i \beta_j \frac{\boldsymbol{\alpha}_j \cdot \mathbf{r}_{jk}}{r_{jk}^3} - \beta_j \boldsymbol{\Sigma}_j \cdot \frac{\boldsymbol{\alpha}_k \times \mathbf{r}_{jk}}{r_{jk}^3} \right). \quad (21)$$

Here, $a_e = \alpha/(2\pi) + \dots$ is the amm of the free electron, and

$$\boldsymbol{\Sigma} = \begin{pmatrix} \boldsymbol{\sigma} & 0 \\ 0 & \boldsymbol{\sigma} \end{pmatrix}.$$

TABLE II. Screened SE correction to the g factor of the ground state of Li-like and B-like ions, in units of 10^{-6} (ppm). “CH,” “KS,” and “LDF” denote results obtained with the core-Hartree, Kohn-Sham, and localized Dirac-Fock potentials, respectively. “AV” denotes the averaged result. For Li-like ions, results obtained by two different methods are presented, namely, the screening-potential approximation (labeled by “scr”) and the combined screening-potential-and-amm approximation (labeled by “scr+amm”). For B-like ions, results obtained by the screening-potential approximation are listed.

Z	Method	CH	KS	LDF	AV
Li-like:					
14	scr	-0.240	-0.258	-0.257 (4)	-0.257 (27)
	scr+amm	-0.250	-0.254	-0.262 (4)	-0.258 (17)
18	scr	-0.326	-0.349	-0.356 (4)	-0.352 (45)
	scr+amm	-0.340	-0.344	-0.363 (4)	-0.354 (35)
20	scr	-0.371	-0.395	-0.409 (4)	-0.402 (58)
	scr+amm	-0.387	-0.390	-0.418 (4)	-0.404 (46)
24	scr	-0.464	-0.491	-0.523 (3)	-0.507 (89)
	scr+amm	-0.485	-0.487	-0.534 (3)	-0.510 (72)
32	scr	-0.661	-0.695	-0.776 (1)	-0.74 (17)
	scr+amm	-0.697	-0.697	-0.792 (1)	-0.75 (14)
54	scr	-1.318	-1.313 (1)	-1.689 (1)	-1.50 (57)
	scr+amm	-1.429	-1.395 (1)	-1.718 (1)	-1.56 (48)
82	scr	-3.007 (1)	-2.599 (1)	-3.897 (1)	-3.2 (1.9)
	scr+amm	-3.249 (1)	-3.199 (1)	-3.900 (1)	-3.6 (1.0)
92	scr	-4.168 (6)	-3.353 (6)	-5.301 (6)	-4.3 (2.9)
	scr+amm	-4.384 (6)	-4.537 (6)	-5.257 (6)	-4.9 (1.3)
B-like:					
18	scr	-1.042 (4)	-0.990 (4)	-0.934 (5)	-0.96 (16)
20	scr	-1.217 (4)	-1.150 (4)	-1.093 (5)	-1.12 (18)
24	scr	-1.621 (4)	-1.528 (3)	-1.467 (5)	-1.50 (23)
32	scr	-2.670 (3)	-2.519 (1)	-2.448 (5)	-2.48 (33)
54	scr	-7.281 (1)	-6.923 (2)	-6.870 (1)	-6.90 (61)
82	scr	-17.374 (1)	-16.383 (1)	-16.843 (1)	-16.61 (1.48)
92	scr	-23.030 (1)	-21.477 (1)	-22.554 (1)	-22.02 (2.33)

To the first order in $1/Z$, the amm correction to the g factor can be expressed as [47]

$$\Delta E_{\text{amm}} = \sum_c [\delta_{H_1} (\langle vc | I_{\text{Breit}} | vc \rangle - \langle cv | I_{\text{Breit}} | vc \rangle) + \delta_{H_2} \delta_{V_{\text{mag}}} (\langle vc | I_{\text{Breit}} | vc \rangle - \langle cv | I_{\text{Breit}} | vc \rangle) + \delta_{V_{\text{mag}}} (\langle vc | H_3 | vc \rangle - \langle cv | H_3 | vc \rangle)], \quad (22)$$

where $\delta_V(\dots)$ denotes the first-order perturbation correction of (\dots) induced by V and I_{Breit} is the electron-electron interaction operator in Eq. (10) in the Breit approximation.

The amm approximation is most suitable for light Li-like ions, whereas for heavy ions the screening-potential approximation becomes preferable. It should be mentioned that for B-like ions, the valence electron is in the $2p_{1/2}$ state and the amm approximation is not applicable at all since it yields only a part of the $(Z\alpha)^2$ contribution, and not a dominant one.

In the present work, we developed a way to combine both the screening-potential and amm approximations (for Li-like ions). To this end, we evaluate the amm correction in Eq. (22) within the screening-potential approximation,

$$\Delta E_{\text{amm}}(\text{scr}) = \delta_{H_1} \langle v | V_{\text{scr}} | v \rangle + \delta_{H_2} \delta_{V_{\text{mag}}} \langle v | V_{\text{scr}} | v \rangle + \delta_{V_{\text{mag}}} \langle v | H_{3,\text{scr}} | v \rangle, \quad (23)$$

where

$$H_{3,\text{scr}} = -ia_e \frac{\alpha}{2} \beta \alpha \cdot \nabla V_{\text{scr}}(r). \quad (24)$$

The difference of Eqs. (23) and (22) gives the amm correction that is *beyond* the screening-potential approximation, which can be added to the results obtained in Sec. III B 1.

C. Self-energy results

The results of our numerical calculations of the screened SE correction for the ground state of Li-like and B-like ions are presented in Table II. For Li-like ions, we present data obtained with two approaches: the screening-potential approximation and the combined screening-potential-and-amm approximation. With each of the two methods, we employed three different screening potentials: the CH, KS, and LDF potentials. The final result was obtained as a half-sum of the KS and LDF values, with the error taken as the maximal difference between the three (CH, KS, and LDF) values, multiplied by a factor of 1.5. This error estimate is supposed to account for uncalculated effects that are beyond the screening-potential approximation. We observe that the combined screening-potential-and-amm approach yields results with a smaller dependence on the choice of the potential and, as a consequence, to smaller error bars. For B-like ions, we present results obtained only with the screening-potential

TABLE III. Comparison of different calculations of the screened SE corrections to the g factor of the ground state of Li-like ions, in ppm.

Z	This work	Full QED [45]	Screening potential [46]	AMM [47]
14	-0.258 (17)	-0.242 (5)		-0.22 (5)
18	-0.354 (35)		-0.24 (8)	-0.29 (8)
20	-0.404 (46)	-0.387 (7)	-0.27 (10)	-0.33 (10)
32	-0.75 (14)		-0.49 (14)	-0.62 (27)
82	-3.6 (1.0)	-3.44 (2)	-3.7 (1.3)	-5.6 (2.0)
92	-4.9 (1.3)	-4.73 (2)	-3.3 (1.2)	-9.2 (2.6)

approximation, since the amm approach is not applicable in this case.

Table III presents a comparison of the results obtained in this work for the screened SE correction for Li-like ions with results of previous calculations [45–47]. We observe good agreement of our data with the results of full QED calculations [45] and some deviations from the results obtained by approximate methods. Our final results for all available SE corrections to the g factor of the ground state of Li-like and B-like ions are listed in Table IV.

IV. VACUUM POLARIZATION

A. One-electron vacuum polarization

In the independent electron approximation, i.e., without taking into account the interactions among the electrons, only the valence electron gives a vacuum polarization (VP) contribution to the Zeeman splitting. The corresponding diagrams are shown in Fig. 4. These diagrams are divided into two groups. The first group comprises the diagrams in Figs. 4(a) and 4(b). They arise due to perturbations of the external wave functions in the tadpole diagram. We call this group

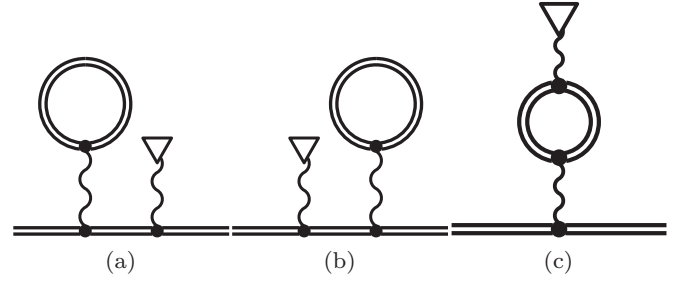


FIG. 4. Feynman diagrams corresponding to the vacuum polarization contributions arising from the interaction of the valence electron.

the electric loop (EL) contributions. The remaining diagram in Fig. 4(c) arises due to a loop correction to the propagator of the photon mediating the magnetic interaction. Accordingly, it is called the magnetic loop (ML) contribution. The total VP contribution to the Zeeman splitting can thus be written as

$$\Delta E_{VP} = \Delta E_{VP,EL} + \Delta E_{VP,ML}. \quad (25)$$

For the computation of the EL contribution, we note that the tadpole part of the EL diagrams is equivalent to the insertion of a potential function U_{EL} called EL potential. A detailed derivation of the formal expression for U_{EL} is given in Ref. [51]. It reads

$$U_{EL}(\mathbf{x}) = \frac{i\alpha}{2\pi} \int d^3y \frac{1}{|\mathbf{x} - \mathbf{y}|} \int_{C_F} d\omega \text{tr}[G(\omega, \mathbf{y}, \mathbf{y})], \quad (26)$$

where, again, G denotes the Dirac Coulomb Green's function and C_F is the usual Feynman integration contour. The contribution to the energy shift is then

$$\Delta E_{VP,EL} = 2\langle v|U_{EL}|\delta v\rangle, \quad (27)$$

where the first-order perturbation $|\delta v\rangle$ of the reference state is given by Eq. (8).

TABLE IV. SE corrections to the g factor of the ground state of Li-like and B-like ions, in ppm. Labeling is as follows: “One-electron (pnt)” denotes hydrogenic point-nucleus SE correction (for the $2s$ state, the results are taken from Ref. [8]), “One-electron (fns)” denotes the finite nuclear size SE correction, and “Screening” denotes the screened SE correction.

Z	One-electron (pnt)	One-electron (fns)	Screening	Total
Li-like:				
14	2324.074 (3)		-0.258 (17)	2323.816 (18)
18	2325.052 (5)		-0.354 (35)	2324.698 (35)
20	2325.674 (5)		-0.404 (46)	2325.270 (47)
24	2327.225 (5)		-0.510 (72)	2326.714 (73)
32	2331.726 (6)	-0.001	-0.75 (14)	2330.98 (14)
54	2358.184 (9)	-0.040	-1.56 (48)	2356.59 (48)
82	2456.245 (9)	-1.540 (1)	-3.55 (1.05)	2451.16 (1.05)
92	2532.207 (9)	-5.488 (6)	-4.90 (1.31)	2521.82 (1.31)
B-like:				
18	-768.3723 (1)		-0.96 (16)	-769.34 (16)
20	-766.7594 (1)		-1.12 (18)	-767.88 (18)
24	-762.7517 (1)		-1.50 (23)	-764.25 (23)
32	-751.0481 (1)	-0.001	-2.48 (33)	-753.53 (33)
54	-683.2643 (1)	-0.012	-6.90 (62)	-690.17 (62)
82	-474.4496 (4)	-0.301	-16.61 (1.49)	-491.36 (1.49)
92	-344.1780 (3)	-1.059 (1)	-22.02 (2.33)	-367.25 (2.33)

The expression in Eq. (26) is divergent and needs to be renormalized. To this end, the potential U_{EL} is expanded in powers of the nuclear coupling strength $Z\alpha$. This corresponds to an expansion of the loop in Figs. 4(a) and in Fig. 4(b) in terms of the free-electron propagator and interactions with the nucleus. Due to Furry's theorem, only odd powers of $Z\alpha$ contribute.

The leading term is of order $Z\alpha$ and is called the Uehling contribution. This term is charge divergent. After renormalization, it results in a finite potential called the Uehling potential and is given by [52]

$$U_{\text{Ue}}(\mathbf{x}) = -\frac{2}{3}\frac{\alpha}{\pi}Z\alpha \int d^3y \frac{\varrho(\mathbf{y})}{|\mathbf{x}-\mathbf{y}|} K_1(2|\mathbf{x}-\mathbf{y}|), \quad (28)$$

where ϱ denotes the nuclear charge distribution normalized to one and where

$$K_1(x) = \int_1^\infty dt e^{-xt} \left(1 + \frac{1}{2t^2}\right) \frac{\sqrt{t^2-1}}{t^2}. \quad (29)$$

For our computations of the Uehling potential, we use analytical formulas resulting from a homogeneously charged sphere as nucleus which have been derived in Ref. [53].

The contribution of higher order in $Z\alpha$ to the EL potential is called the Wichmann-Kroll potential U_{WK} [54]. We use the expressions in Ref. [51] to obtain a partial-wave expansion for the contributions to the g factor from the partial-wave expansion of the Wichmann-Kroll potential given by

$$U_{\text{WK}}(\mathbf{x}) = \sum_{|\kappa|=1}^{\infty} U_{\text{WK}}^{|\kappa|}(\mathbf{x}). \quad (30)$$

We truncate the partial-wave expansion of the g factor at a finite value of $|\kappa|$, typically $|\kappa| = 11$, and estimate the remainder by fitting polynomials in $1/|\kappa|$ to the tail of the partial-wave contributions. In Ref. [51] the nucleus is taken to be a spherical shell and analytical solutions for the Dirac-Coulomb Green's function are used in the calculations. We, however, use a homogeneously charged sphere as a nucleus and, thus, compute the Dirac-Coulomb Green's function numerically, much in the spirit of Refs. [43,49]. The numerical calculation is performed using the method of Refs. [55,56] for solving the stationary Dirac equation. We also use approximate expressions for this potential derived in Ref. [57] for pointlike nuclei to check our numerical calculations. The total EL potential is then

$$U_{\text{EL}} = U_{\text{Ue}} + U_{\text{WK}}. \quad (31)$$

In the case of the ML contribution, the effect of the loop can be expressed as a modification of the vector potential of the external magnetic field. This results in a modification of V_{mag} to V_{ML} and the contribution to the Zeeman splitting is given by

$$\Delta E_{\text{VP,ML}} = \langle v|V_{\text{ML}}|v\rangle, \quad (32)$$

where $V_{\text{ML}} = -e\boldsymbol{\alpha} \cdot \mathbf{A}_{\text{ML}}$ and \mathbf{A}_{ML} is the modified vector potential.

In order to compute the modified vector potential, the loop is, again, expanded in terms of the free-electron propagator and interactions with the nuclear field. The leading order term for a pointlike nucleus is $\propto (Z\alpha)^2$ and has been derived in

Refs. [6,58]. We call this term the Delbrück contribution. We only take this leading order term into account and neglect higher-order contributions as we expect them to be small compared to the uncertainties of other contributions to the g factor. We obtain

$$\mathbf{A}_{\text{ML}}(\mathbf{r}) = \mathbf{A}(\mathbf{r})\Pi_{\text{De}}(|\mathbf{r}|), \quad (33)$$

where the polarization function Π_{De} is given by

$$\Pi_{\text{De}}(x) = \frac{\alpha}{\pi}(Z\alpha)^2 \frac{4}{x^2} \int_0^\infty dq F_{\text{De}}(q) j_1(qx) qx. \quad (34)$$

In this formula, j_1 is the spherical Bessel function of order one and the function F_{De} is taken from Ref. [58]. In Tables VII and VIII we estimate the uncertainty of the ML contribution due to higher-order contributions conservatively to be $(Z\alpha)^2 \ln[(Z\alpha)^{-2}]$ times the Delbrück contribution and include this into the calculation of the uncertainty of the one-electron VP contribution.

B. First-order screened vacuum polarization

Apart from single-electron VP contributions to the bound-electron g factor, we calculated the leading order interelectronic-interaction correction to the VP effect. Typical examples of the corresponding Feynman diagrams are depicted in Fig. 5. Each of these diagrams represents one of four groups of contributions.

The first group of contributions is again called electric loop contributions. The diagram in Fig. 5(a) depicts one of the diagrams belonging to this group. These EL contributions arise due to first-order perturbative corrections to the wave functions of the external and the intermediate states and to the energy levels of the electronic states. Again, there are reducible and irreducible contributions to the Zeeman splitting. Expressions for these contributions have been derived for Li-like systems in Ref. [59] using the two-time Green's function formalism [30], which can be readily generalized to the B-like case. Alternatively, one can start from Eqs. (9) and (11) and systematically consider the perturbations of each of the matrix elements. This approach has the additional advantage that it also provides a numerical algorithm to evaluate the contributions. We used this second approach to verify the formulas of Ref. [59] and to compute these contributions.

The second group of contributions, represented by the diagram in Fig. 5(b) with a loop on the photon mediating the magnetic interaction, is correspondingly called the magnetic loop contributions. To compute these contributions, we need to substitute the magnetic potential V_{mag} in Eq. (8) by the magnetic loop potential V_{ML} which arises from the modified vector potential in Eq. (33).

The third group of contributions, represented by Fig. 5(c), arises from a loop correction to the photon propagator mediating the interaction between the electrons. Accordingly, we call it the electric loop propagator (ELP) contributions. We expand the loop in terms of the free-electron propagator and interactions with the nuclear potential. We take again only the leading order term into account, which is just the free-electron loop, since higher-order contributions are expected to be smaller than the uncertainties of other contributions. This modifies the photon interaction operator I from Eq. (10)

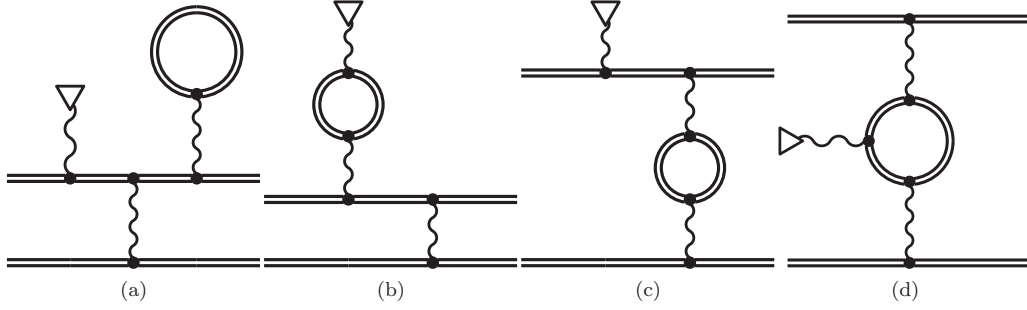


FIG. 5. Vacuum polarization contributions to the two-electron interaction. Each of the diagrams shown represents one type of contribution. Contributions represented by the first diagram are called electric loop (EL), by the second diagram magnetic loop (ML), by the third diagram electric loop propagator (ELP), and by the fourth magnetic loop propagator (MLP) contributions.

into [60,61]

$$\tilde{I}(\varepsilon, \mathbf{r}_1, \mathbf{r}_2) = \frac{2}{3} \frac{\alpha}{\pi} \int_1^\infty dt \left(1 + \frac{1}{2t^2}\right) \frac{\sqrt{t^2 - 1}}{t^2} \times I(\sqrt{\varepsilon^2 - (2t)^2}, \mathbf{r}_1, \mathbf{r}_2). \quad (35)$$

The contribution is then obtained by using \tilde{I} instead of I in Eqs. (9) and (11).

The fourth group of contributions is called magnetic loop propagator (MLP) contributions. The diagram in Fig. 5(d) represents one of the contributing diagrams. If we expand this diagram in terms of the free-electron propagator and interactions with the nuclear field, then, due to Furry's theorem, the leading-order contribution will have four vertices. As such, its leading contribution is of higher order than the ELP contribution. Thus, we neglect these terms anticipating that their contribution will be small.

Higher-order interaction effects (i.e., of order $1/Z^2$ or higher) have been estimated and given as uncertainty of the first-order screened vacuum polarization result. For Li-like ions, this effect has been calculated using a screening-potential approach. For B-like ions, we expect these terms of higher order to be too small to be visible compared to the uncertainties of the other contributions for most of the ions considered in this work. Thus, we estimate the uncertainty due to higher-order contributions to be 10% of the first-order contributions.

C. Vacuum polarization results

We present our results of the single-electron VP correction for the ground state of Li-like and B-like ions in Table V. The contributions are divided into EL and ML contributions according to our discussion above. The Uehling and Wichmann-Kroll contributions to the EL term are listed separately. Both contributions are calculated taking the nuclear size into account. The uncertainties result from the quoted uncertainties of the rms radii in Ref. [33]. Compared to the uncertainties of the other contributions to the g factor, we expect the dependence on the nuclear model of higher-order corrections to be of no relevance. In the case of the Wichmann-Kroll contributions, the uncertainties additionally include the uncertainties from the truncation of the partial-wave expansion. The Delbrück contribution has been calculated for a pointlike nucleus using the formulas of Refs. [6,58]. We observe that

the Uehling terms are the largest contributions in magnitude for both the Li-like and the B-like case. In the Li-like case, we see that while the Delbrück contribution is larger than the Wichmann-Kroll contribution for low nuclear charges, this changes for higher nuclear charges. We also observe that in the B-like case the Uehling and Delbrück contributions cancel each other to a significant degree for low nuclear charges.

In addition, we compared our numerical results for the Uehling VP correction with the $Z\alpha$ expansion. In Ref. [62], a $Z\alpha$ expansion formula for the Uehling correction was derived up to order $(Z\alpha)^7$ for the $1s$ state only. We derived an approximation formula for the Uehling correction in the $2p_{1/2}$ state using nonrelativistic expansions of both the bound-electron wave functions and the wave functions perturbed linearly by a magnetic field (see Ref. [63] for the derivation of the perturbed wave function). The formula for the Uehling correction is

$$g_{Ue,2p} = \frac{8}{3} \int dr U_{Ue}(r) [G_{2p}(r)X_{2p}(r) + F_{2p}(r)Y_{2p}(r)], \quad (36)$$

with the radial components of the bound-electron wave function G_{2p} and F_{2p} and the magnetic wave function X_{2p} and Y_{2p} . For the $2p_{1/2}$ state, we find the following nonrelativistic expansions of the wave functions:

$$G_{2p}(r) \approx - \left(\frac{Z\alpha}{2}\right)^{1/2} \frac{(Z\alpha r)^2}{2\sqrt{3}} \exp\left(-\frac{Z\alpha r}{2}\right), \quad (37)$$

$$F_{2p}(r) \approx - \left(\frac{Z\alpha}{2}\right)^{3/2} \frac{3Z\alpha r}{2\sqrt{3}} \exp\left(-\frac{Z\alpha r}{2}\right). \quad (38)$$

For the radial components of the magnetic wave function, we find

$$X_{2p}(r) \approx \frac{3}{2} r F_{2p}(r) - \frac{1}{2} G_{2p}(r), \quad (39)$$

$$Y_{2p}(r) \approx \frac{1}{2} r G_{2p}(r) + \frac{3}{2} F_{2p}(r), \quad (40)$$

using $E_{2p} = 1 + O[(Z\alpha)^2]$. With these nonrelativistic wave functions, the radial integration in Eq. (36) as well as the remaining integration in the representation of the Uehling potential [64] were carried out analytically to obtain

$$g_{Ue,2p} \approx -\frac{31}{840} \frac{\alpha}{\pi} (Z\alpha)^6. \quad (41)$$

We would like to point out that one has to employ the exact representation of the Uehling potential in the derivation of this

TABLE V. Single-electron VP corrections to the g factor of the ground state of Li-like and B-like ions, in units of ppm. The uncertainty of the Uehling contribution results from the uncertainty of the nuclear rms taken from Ref. [33]. The uncertainty of the Wichmann-Kroll contribution is the combined uncertainty due to the nuclear rms and the extrapolation of the partial-wave series.

Z	EL, Uehling	EL, Wichmann-Kroll	ML, Delbrück
Li-like:			
18	-0.080 041 83 (2)	0.000 244 93 (4)	0.001 102 6
20	-0.120 944 51 (3)	0.000 448 74 (4)	0.001 850 7
24	-0.247 384 1 (2)	0.001 275 7 (1)	0.004 524 6
32	-0.771 498 4 (4)	0.006 605 (4)	0.018 438
54	-6.622 35 (5)	0.134 88 (1)	0.234 30
82	-46.814 5 (4)	1.754 1(1)	1.796 6
92	-87.661 (4)	3.796 7(3)	3.168
B-like:			
18	-0.000 418 694 19 (2)	0.000 002 44 (3)	0.000 413 11
20	-0.000 789 094 95 (4)	0.000 005 49 (5)	0.000 706 75
24	-0.002 372 519 (1)	0.000 022 4 (1)	0.001 797 2
32	-0.013 710 925 (2)	0.000 209 (3)	0.007 950 5
54	-0.376 778 (1)	0.012 93 (2)	0.128 97
82	-7.250 91 (4)	0.444 58(5)	1.410 8
92	-18.394 5 (3)	1.289 7(1)	2.881 5

formula since we would obtain the incomplete result

$$g_{\text{Ue},2p,\text{incomplete}} \approx -\frac{1}{40} \frac{\alpha}{\pi} (Z\alpha)^6 \quad (42)$$

by using the δ function approximation of the Uehling potential. For the $1s$ state, however, the δ function approximation of the Uehling potential is sufficient to derive the well-known lowest-order contribution to the Uehling correction (e.g., [62]),

$$g_{\text{Ue},1s} \approx -\frac{16}{15} \frac{\alpha}{\pi} (Z\alpha)^4. \quad (43)$$

Our numerical all-order results for the Uehling correction were found to be in good agreement with the approximation formula in Eq. (41) for low Z .

The results for the first-order screened VP corrections for the ground state of Li-like and B-like ions are listed in Table VI. The contributions are divided according to the groups of diagrams discussed above. Compared to the single-electron case, we have additionally the ELP contribution. This has been calculated using the leading free-electron contribution.

V. OTHER EFFECTS

A. Nuclear recoil

In Furry picture calculations, the nucleus is taken to be a source of a classical background electric field. This corresponds to taking the nuclear mass M to be infinite. While this often gives a reasonably accurate first approximation, one needs to take the finite mass of the nucleus into account for more precise computations of the bound-electron g factor. This is done in a perturbative expansion in the small parameter $1/M$.

In this paper, we include for completeness results for the nuclear-recoil effect to order $1/M$ calculated and tabulated in Ref. [65] for Li-like ions, and in Refs. [66,67] for B-like ions.

We note that the calculations of the nuclear recoil effect for B-like ions have been improved very recently in Ref. [68]. No values were tabulated for Li-like Xe^{51+} and B-like Cr^{19+} , Ge^{27+} , and Xe^{49+} in the given references. For these ions, we obtained values and corresponding uncertainties by fitting functions to the tabulated values, as explained in the following.

For Li- as well as B-like ions, the nuclear recoil correction to the g factor is written as the sum of a Breit term Δg_{Breit} and a QED term Δg_{QED} . For Li-like ions, the Breit term is parametrized in Ref. [65] as

$$\Delta g_{\text{rec,Breit}} = \frac{(Z\alpha)^2}{M} \left[A(Z\alpha) + \frac{B(Z\alpha)}{Z} + \frac{C(Z\alpha, Z)}{Z^2} \right], \quad (44)$$

where the coefficients $A(Z\alpha)$ and $B(Z\alpha)$ denote contributions of zeroth and first order in $1/Z$, respectively, and $C(Z\alpha, Z)$ denotes contributions of second and higher order in $1/Z$. The coefficient $A(Z\alpha)$ was calculated analytically while $B(Z\alpha)$ and $C(Z\alpha, Z)$ were calculated and tabulated numerically in the given reference. The QED part is parametrized as

$$\Delta g_{\text{rec,QED}} = \frac{1}{M} \frac{(Z\alpha)^5}{8} P(Z\alpha). \quad (45)$$

Interelectronic interaction corrections were included using screening-potential approximations. To obtain values for Xe^{51+} , we proceeded as follows: We calculated $A(Z\alpha)$ using the analytical formula given in Ref. [65]. For $B(Z\alpha)$ and $C(Z\alpha, Z)$, we fitted polynomials in $Z\alpha$ to the tabulated values in the reference. We use the $a + b(Z\alpha)^2 + c(Z\alpha)^4$ to fit $B(Z\alpha)$ and $a + b(Z\alpha) + c(Z\alpha)^2 + d(Z\alpha)^3$ to fit $Z\alpha C(Z\alpha, Z)$. For the QED part, given by $Z\alpha P(Z\alpha)$, we used the function $a \ln(Z\alpha) + b + c(Z\alpha) + d(Z\alpha)^5$.

For B-like ions, the Breit term is parametrized in Refs. [66,67] as

$$\Delta g_{\text{rec,Breit}} = \frac{1}{M} \left[A_L(Z\alpha) + \frac{B(Z\alpha)}{Z} \right], \quad (46)$$

TABLE VI. First-order VP screening correction to the g factor of the ground state of Li-like and B-like ions, in units of ppm. The uncertainty of the Uehling contribution results from the uncertainty of the nuclear rms taken from Ref. [33]. The uncertainty of the Wichmann-Kroll contribution is the combined uncertainty due to the nuclear rms and the extrapolation of the partial-wave series.

Z	EL, Uehling	EL, Wichmann-Kroll	ELP, Uehling	ML, Delbrück
Li-like:				
18	0.012 746 390(3)	−0.000 038 987 (5)	−0.000 085 6	−0.000 163 3
20	0.017 346 904(4)	−0.000 064 318 (7)	−0.000 118	−0.000 246 8
24	0.029 614 54(3)	−0.000 152 52 (1)	−0.000 205	−0.000 503 0
32	0.069 500 41(3)	−0.000 593 2 (3)	−0.000 499	−0.001 537
54	0.356 946(3)	−0.007 203 3(5)	−0.002 71	−0.011 5
82	1.676 36(2)	−0.061 650 (4)	−0.014	−0.056
92	2.800 2(2)	−0.118 67 (2)	−0.024	−0.085
B-like:				
18	0.006 522(2)	−0.000 021 16 (1)	0.000 003 6	−0.000 134 1
20	0.008 987(2)	−0.000 035 59 (2)	0.000 011	−0.000 207
24	0.015 766(2)	−0.000 088 00 (7)	0.000 044	−0.000 443
32	0.039 435(5)	−0.000 374 (2)	0.000 26	−0.001 499
54	0.257 1(2)	−0.006 256 (7)	0.005 0	−0.015 5
82	1.853(2)	−0.088 1 (1)	0.059	−0.126
92	3.728(2)	−0.206 8 (3)	0.13	−0.24

where the coefficients $A_L(Z\alpha)$ and $B(Z\alpha)$ again denote contributions of zeroth and first order in $1/Z$, respectively. The subscript “L” on the coefficient denotes that only lower-order terms in $Z\alpha$ are included. The QED part is given as

$$\Delta g_{\text{rec,QED}} = \frac{1}{M} \left[A_{\text{H}}^{2\text{el}}(Z\alpha) + \frac{(Z\alpha)^3}{8} P(Z\alpha) \right], \quad (47)$$

where the subscript H denotes higher-order terms in $Z\alpha$ and the superscript “2el” denotes two-electron contributions to the recoil correction. Again, interelectronic interactions are included using screening-potential approximations. To obtain the recoil correction for Ca^{15+} , Cr^{19+} , and Xe^{49+} , we fit the function $a + b(Z\alpha)^2 + c(Z\alpha)^3 + d(Z\alpha)^7$ to the data for $Z\alpha[A_L(Z\alpha) + B(Z\alpha)/Z]$ tabulated in Refs. [66,67], the function $a + b(Z\alpha)^2 + c(Z\alpha)^4 + d(Z\alpha)^6$ to the values for $A_{\text{H}}^{2\text{el}}(Z\alpha)$, and the function $a + bZ\alpha + c(Z\alpha)^2$ to the data for $Z\alpha P(Z\alpha)$ for small values of Z tabulated in Ref. [67].

B. Two-loop effects

For the calculation of two-loop contributions in the independent electron approximation, we use formulas from Refs. [34,69]. These formulas assume a pointlike nucleus and are perturbative in the nuclear-coupling strength $Z\alpha$.

In the Li-like case, the formula includes terms up to order $(Z\alpha)^2$ and reads [34]

$$g_{2s,\text{two-loop}} = -2 \left[1 + \frac{1}{24} (Z\alpha)^2 \right] C_4 \left(\frac{\alpha}{\pi} \right)^2, \quad (48)$$

where C_4 denotes the coefficient of the $(\alpha/\pi)^2$ contribution in the expansion of the free-electron magnetic anomaly a_e . The expansion coefficient is taken from Ref. [70]. Uncertainties from higher-order contributions are estimated by using the formula for the $(Z\alpha)^4$ contribution from Ref. [4].

For B-like systems, we have an analytic expression to order $(Z\alpha)^0$. It is given by [69]

$$g_{2p_{1/2},\text{two-loop}} = -\frac{2}{3} C_4 \left(\frac{\alpha}{\pi} \right)^2. \quad (49)$$

We estimate the uncertainty due to terms of higher order in $Z\alpha$ following the method of Ref. [4] as

$$g_{\text{h.o.}}^{(2)} = 2g_{\text{h.o.}}^{(1)} \frac{g^{(2)}[(Z\alpha)^0]}{g^{(1)}[(Z\alpha)^0]}, \quad (50)$$

where $g_{\text{h.o.}}^{(n)}$ is the n -loop higher-order QED contribution and $g^{(n)}[(Z\alpha)^0]$ is the n -loop $(Z\alpha)^0$ QED contribution. The contribution $g_{\text{h.o.}}^{(1)}$ as well as the contributions of order $(Z\alpha)^0$ are calculated with the formulas of Ref. [69].

VI. RESULTS AND SUMMARY

In Tables VII and VIII we present numerical results for all the contributions discussed in this work, for Li-like and B-like ions, respectively. In Table VII, we include previous results for the total g factor of Li-like ions from Refs. [45,47] for comparison. Our results independently confirm these calculations within the given uncertainties. Our results feature a smaller uncertainty for high- Z ions than the results of Ref. [47] from 2004 due to an improved calculation of the screened self-energy contributions by the combination of the screening potential and the amm methods. We also include screened vacuum-polarization contributions which become visible in the high- Z regime. Reference [45] treats many-electron QED effects rigorously by the evaluation of the corresponding photon exchange QED screening diagrams and two-photon exchange diagrams, and thus provides the most precise results for the few atomic numbers considered therein. Our value for the g factor of $^{40}\text{Ca}^{17+}$ agrees also with the experimental value

$$g_{\text{expt.}}(^{40}\text{Ca}^{17+}) = 1.999\,202\,040\,5(11)$$

from Ref. [71] within the given uncertainties.

TABLE VII. Contributions to the bound-electron g factor of lithiumlike ions. The uncertainties given in parentheses indicate the uncertainty of the last digit(s). If no uncertainty is given, all digits of the quoted value are significant.

Contribution	$^{40}\text{Ar}^{15+}$	$^{40}\text{Ca}^{17+}$	$^{52}\text{Cr}^{21+}$	$^{74}\text{Ge}^{29+}$
Dirac value	1.997 108 8	1.996 426 0	1.994 838 1	1.990 752 3
Finite nuclear size	0.000 000 0	0.000 000 0	0.000 000 0	0.000 000 2
Electron correlation:				
one-photon exchange, $(1/Z)^1$	0.000 414 5	0.000 461 1	0.000 555 2	0.000 746 5
$(1/Z)^{2+}$, CI-DFS	-0.000 006 7(2)	-0.000 006 7(2)	-0.000 006 7(2)	-0.000 006 7(3)
Nuclear recoil	0.000 000 1	0.000 000 1	0.000 000 1	0.000 000 1
One-loop QED:				
SE, $(1/Z)^0$	0.002 325 1	0.002 325 7	0.002 327 2	0.002 331 7
SE, $(1/Z)^{1+}$	-0.000 000 4(1)	-0.000 000 4(1)	-0.000 000 5(1)	-0.000 000 8(2)
VP, $(1/Z)^0$	-0.000 000 1	-0.000 000 1	-0.000 000 2	-0.000 000 8
VP, $(1/Z)^{1+}$	0.000 000 0	0.000 000 0	0.000 000 0	0.000 000 1
Two-loop QED	-0.000 003 5	-0.000 003 5	-0.000 003 5	-0.000 003 6(2)
Total theory	1.999 837 8(2)	1.999 202 2(2)	1.997 709 7(2)	1.993 819 0(4)
Theory, Ref. [47]	1.999 837 75(14)	1.999 202 24(17)	1.997 709 70(26)	1.993 819 14(46)
Theory, Ref. [45]		1.999 202 041(13)		
Contribution	$^{132}\text{Xe}^{51+}$	$^{208}\text{Pb}^{79+}$	$^{238}\text{U}^{89+}$	
Dirac value	1.972 750 2	1.932 002 9	1.910 723	
Finite nuclear size	0.000 003 4	0.000 078 7(1)	0.000 242	
Electron correlation:				
one-photon exchange, $(1/Z)^1$	0.001 306 2	0.002 148 3	0.002 510	
$(1/Z)^{2+}$, CI-DFS	-0.000 006 8(3)	-0.000 007 6(4)	-0.000 008(1)	
Nuclear recoil	0.000 000 2	0.000 000 4	0.000 001	
One-loop QED:				
SE, $(1/Z)^0$	0.002 358 1(1)	0.002 454 7	0.002 527	
SE, $(1/Z)^{1+}$	-0.000 001 6(5)	-0.000 003 6(11)	-0.000 005(1)	
VP, $(1/Z)^0$	-0.000 006 3(1)	-0.000 043 2(7)	-0.000 081(1)	
VP, $(1/Z)^{1+}$	0.000 000 3(1)	0.000 001 6(1)	0.000 003(1)	
Two-loop QED	-0.000 003 6(2)	-0.000 003 6(12)	-0.000 004(2)	
Total theory	1.976 400 1(6)	1.936 628 6(18)	1.915 908(3)	
Theory, Ref. [47]	1.976 399 9(14)	1.936 625 3(35)	1.915 900 2(50)	
Theory, Ref. [45]		1.936 627 2(6)	1.915 904 8(11)	

For low atomic numbers, i.e., lower than those considered here, the nonrelativistic QED approach employing explicitly correlated three-electron wave functions was found to improve the overall theoretical uncertainty [72]. For Li-like $^{28}\text{Si}^{11+}$, the most precise experimental and theoretical g -factor values can be found in the very recent Ref. [73].

In Table VIII, we include previous results for the total g factor of B-like ions from Refs. [38,39,74,75]. Our results confirm the calculations of Refs. [38,39] within the uncertainties. We have improved the uncertainties compared to these works due to an improved treatment of the self-energy contributions.

Recently, the g factor of B-like $^{40}\text{Ar}^{13+}$ was measured by the ALPHATRAP experiment [76] at the Max Planck Institute for Nuclear Physics [29]. The experiment constitutes the first high-precision measurement of the bound-electron g factor of a B-like ion, greatly improving the previous experimental value [77]. The measured value for $^{40}\text{Ar}^{13+}$ is [29]

$$g_{\text{expt.}}(^{40}\text{Ar}^{13+}) = 0.663\,648\,455\,32\,(93).$$

Within the given uncertainty, this value agrees with our result listed in Table VIII. Our calculation in this work agrees also with a combined theoretical value $g(^{40}\text{Ar}^{13+}) = 0.663\,648\,12\,(58)$ of Ref. [29].

Currently, the main limitation for the calculation of the g factor of B-like argon stems from the contribution resulting from the higher-order interelectronic interactions. For heavy ions (from Xe^{49+} on), the uncertainties of the screened self-energy contribution dominate over the other uncertainties. Also, vacuum-polarization effects become more visible and need to be taken into account. Accordingly, the results for the g factors of B-like ions can be improved by calculating two-photon exchange contributions (as has been done in Ref. [45] for Li-like ions) and by rigorously calculating the screened self-energy effects (as has been done in Refs. [45,59] for Li-like ions). Furthermore, for a significant increase of the theoretical precision in the case of the heaviest elements such as Pb^{77+} and U^{87+} , which are relevant for an improved determination of the fine-structure constant α , two-loop contributions need to be calculated nonperturbatively in the nuclear-coupling strength $Z\alpha$. First milestones have been achieved for the $1s$ ground state of hydrogenlike systems in Refs. [14,15];

TABLE VIII. Contributions to the bound-electron g factor of boronlike ions. The uncertainties given in parentheses indicate the uncertainty of the last digit(s). If no uncertainty is given, all digits of the quoted value are significant.

Contribution	$^{40}\text{Ar}^{13+}$	$^{40}\text{Ca}^{15+}$	$^{52}\text{Cr}^{19+}$	$^{74}\text{Ge}^{27+}$
Dirac value	0.663 775 5	0.663 092 7	0.661 504 7	0.657 419 0
Finite nuclear size	0.000 000 0	0.000 000 0	0.000 000 0	0.000 000 0
Electron correlation:				
one-photon exchange, $(1/Z)^1$	0.000 657 5	0.000 732 0	0.000 882 4	0.001 190 3
$(1/Z)^{2+}$, CI-DFS	−0.000 007 6(4)	−0.000 007 7(4)	−0.000 008 2(5)	−0.000 011 2(7)
Nuclear recoil	−0.000 009 1(2)	−0.000 009 3(2)	−0.000 007 3	−0.000 005 3
One-loop QED:				
SE, $(1/Z)^0$	−0.000 768 4	−0.000 766 8	−0.000 762 8	−0.000 751 1
SE, $(1/Z)^{1+}$	−0.000 001 0(2)	−0.000 001 1(2)	−0.000 001 5(2)	−0.000 002 5(3)
VP, $(1/Z)^0$	−0.000 000 0	−0.000 000 0	−0.000 000 0	−0.000 000 0
VP, $(1/Z)^{1+}$	0.000 000 0	0.000 000 0	0.000 000 0	0.000 000 0
Two-loop QED	0.000 001 2(1)	0.000 001 2(1)	0.000 001 2(1)	0.000 001 2(1)
Total theory	0.663 648 1(5)	0.663 041 0(5)	0.661 608 5(5)	0.657 840 4(8)
Theory, Ref. [38]	0.663 648 8(12)	0.663 041 8(12)		
Theory, Ref. [39]	0.663 647 7(7)			
Theory, Ref. [74]	0.663 899(2)	0.663 325(56)	0.661 955(68)	0.658 314(93)
Theory, Ref. [75]	0.663 728	0.663 130	0.661 714	
Contribution	$^{132}\text{Xe}^{49+}$	$^{208}\text{Pb}^{77+}$	$^{238}\text{U}^{87+}$	
Dirac value	0.639 416 9	0.598 669 6	0.577 389	
Finite nuclear size	0.000 000 1	0.000 006 8	0.000 029	
Electron correlation:				
one-photon exchange, $(1/Z)^1$	0.002 118 2	0.003 654 9	0.004 394	
$(1/Z)^{2+}$, CI-DFS	−0.000 011 0(5)	−0.000 019 9(7)	−0.000 023	
Nuclear recoil	−0.000 003 0	−0.000 001 8	−0.000 001	
One-loop QED:				
SE, $(1/Z)^0$	−0.000 683 3	−0.000 474 8	−0.000 345	
SE, $(1/Z)^{1+}$	−0.000 006 9(6)	−0.000 016 6(15)	−0.000 022(2)	
VP, $(1/Z)^0$	−0.000 000 2(1)	−0.000 005 5(5)	−0.000 014(1)	
VP, $(1/Z)^{1+}$	0.000 000 2(1)	0.000 001 7(2)	0.000 003(1)	
Two-loop QED	0.000 001 2(1)	0.000 001 2(3)	0.000 001(1)	
Total theory	0.640 832 2(8)	0.601 815 6(18)	0.581 411(3)	
Theory, Ref. [74]	0.641 61(18)	0.602 86(33)	0.582 48(40)	

these calculations need to be extended to the $2p$ valence electron of B-like ions.

In summary, we performed a systematic calculation of interelectronic and radiative effects on the one-loop level to the ground-state g factor of Li-like and B-like ions. These calculations for B-like ions have been extended to heavy elements. The interelectronic interaction on the level of one-photon exchange has been calculated using perturbation theory. Many-electron SE effects have been taken into account through screening potentials while the leading-order screening effect for VP corrections has been calculated explicitly

using perturbation theory. Estimated theoretical uncertainties have been supplemented for each value.

ACKNOWLEDGMENTS

This work is part of and supported by the German Research Foundation (DFG) Collaborative Research Centre “SFB 1225 (ISOQUANT).” The work of V.A.Y. was supported by the Russian Science Foundation (Grant No. 20-62-46006). I.I.T. acknowledges support by the Russian Science Foundation under Grant No. 19-12-00157.

- [1] S. Sturm, A. Wagner, B. Schabinger, J. Zatorski, Z. Harman, W. Quint, G. Werth, C. H. Keitel, and K. Blaum, *Phys. Rev. Lett.* **107**, 023002 (2011).
- [2] S. Sturm, A. Wagner, M. Kretzschmar, W. Quint, G. Werth, and K. Blaum, *Phys. Rev. A* **87**, 030501(R) (2013).
- [3] K. Pachucki, U. D. Jentschura, and V. A. Yerokhin, *Phys. Rev. Lett.* **93**, 150401 (2004).
- [4] K. Pachucki, A. Czarnecki, U. D. Jentschura, and V. A. Yerokhin, *Phys. Rev. A* **72**, 022108 (2005).
- [5] S. G. Karshenboim and A. I. Milstein, *Phys. Lett. B* **549**, 321 (2002).
- [6] R. N. Lee, A. I. Milstein, I. S. Terekhov, and S. G. Karshenboim, *Phys. Rev. A* **71**, 052501 (2005).
- [7] V. A. Yerokhin, P. Indelicato, and V. M. Shabaev, *Phys. Rev. Lett.* **89**, 143001 (2002).
- [8] V. A. Yerokhin, P. Indelicato, and V. M. Shabaev, *Phys. Rev. A* **69**, 052503 (2004).

- [9] V. M. Shabaev and V. A. Yerokhin, *Phys. Rev. Lett.* **88**, 091801 (2002).
- [10] T. Beier, *Phys. Rep.* **339**, 79 (2000).
- [11] T. Beier, I. Lindgren, H. Persson, S. Salomonson, P. Sunnergren, H. Häffner, and N. Hermanspahn, *Phys. Rev. A* **62**, 032510 (2000).
- [12] A. Czarnecki, M. Dowling, J. Piclum, and R. Szafron, *Phys. Rev. Lett.* **120**, 043203 (2018).
- [13] K. Pachucki and M. Puchalski, *Phys. Rev. A* **96**, 032503 (2017).
- [14] V. A. Yerokhin and Z. Harman, *Phys. Rev. A* **88**, 042502 (2013).
- [15] B. Sikora, V. A. Yerokhin, N. S. Oreshkina, H. Cakir, C. H. Keitel, and Z. Harman, *Phys. Rev. Res.* **2**, 012002 (2020).
- [16] S. Sturm, F. Köhler, J. Zatorski, A. Wagner, Z. Harman, G. Werth, W. Quint, C. H. Keitel, and K. Blaum, *Nature (London)* **506**, 467 (2014).
- [17] F. Köhler, S. Sturm, A. Kracke, G. Werth, W. Quint, and K. Blaum, *J. Phys. B* **48**, 144032 (2015).
- [18] J. Zatorski, B. Sikora, S. G. Karshenboim, S. Sturm, F. Köhler-Langes, K. Blaum, C. H. Keitel, and Z. Harman, *Phys. Rev. A* **96**, 012502 (2017).
- [19] D. A. Glazov and V. M. Shabaev, *Phys. Lett. A* **297**, 408 (2002).
- [20] A. V. Nefiodov, G. Plunien, and G. Soff, *Phys. Rev. Lett.* **89**, 081802 (2002).
- [21] J. Zatorski, N. S. Oreshkina, C. H. Keitel, and Z. Harman, *Phys. Rev. Lett.* **108**, 063005 (2012).
- [22] S. Sturm, G. Werth, and K. Blaum, *Ann. Phys. (NY)* **525**, 620 (2013).
- [23] W. Quint, J. Dilling, S. Djekic, H. Häffner, N. Hermanspahn, H.-J. Kluge, G. Marx, R. Moore, D. Rodriguez, J. Schönfelder, G. Sikler, T. Valenzuela, J. Verdú, C. Weber, and G. Werth, *Hyperfine Interact.* **132**, 453 (2001).
- [24] H.-J. Kluge, T. Beier, K. Blaum, L. Dahl, S. Eliseev, F. Herfurth, B. Hofmann, O. Kester, S. Koszudowski, C. Kozhuharov *et al.*, *Adv. Quantum Chem.* **53**, 83 (2008).
- [25] V. M. Shabaev, D. A. Glazov, N. S. Oreshkina, A. V. Volotka, G. Plunien, H.-J. Kluge, and W. Quint, *Phys. Rev. Lett.* **96**, 253002 (2006).
- [26] V. A. Yerokhin, E. Berseneva, Z. Harman, I. I. Tupitsyn, and C. H. Keitel, *Phys. Rev. Lett.* **116**, 100801 (2016).
- [27] V. A. Yerokhin, E. Berseneva, Z. Harman, I. I. Tupitsyn, and C. H. Keitel, *Phys. Rev. A* **94**, 022502 (2016).
- [28] A. V. Volotka and G. Plunien, *Phys. Rev. Lett.* **113**, 023002 (2014).
- [29] I. Arapoglou, A. Egl, M. Höcker, T. Sailer, B. Tu, A. Weigel, R. Wolf, H. Cakir, V. A. Yerokhin, N. S. Oreshkina, V. A. Agababae, A. V. Volotka, D. V. Zinenko, D. A. Glazov, Z. Harman, C. H. Keitel, S. Sturm, and K. Blaum, *Phys. Rev. Lett.* **122**, 253001 (2019).
- [30] V. Shabaev, *Phys. Rep.* **356**, 119 (2002).
- [31] G. Breit, *Nature (London)* **122**, 649 (1928).
- [32] S. A. Zapryagaev, *Opt. Spectrosc.* **47**, 9 (1979).
- [33] I. Angeli and K. Marinova, *At. Data Nucl. Data Tables* **99**, 69 (2013).
- [34] V. M. Shabaev, D. A. Glazov, M. B. Shabaeva, V. A. Yerokhin, G. Plunien, and G. Soff, *Phys. Rev. A* **65**, 062104 (2002).
- [35] W. R. Johnson, S. A. Blundell, and J. Sapirstein, *Phys. Rev. A* **37**, 307 (1988).
- [36] V. M. Shabaev, I. I. Tupitsyn, V. A. Yerokhin, G. Plunien, and G. Soff, *Phys. Rev. Lett.* **93**, 130405 (2004).
- [37] D. A. Glazov, A. V. Volotka, A. A. Schepetnov, M. M. Sokolov, V. M. Shabaev, I. I. Tupitsyn, and G. Plunien, *Phys. Scr.* **T156**, 014014 (2013).
- [38] V. A. Agababae, D. A. Glazov, A. V. Volotka, D. V. Zinenko, V. M. Shabaev, and G. Plunien, *J. Phys. Conf. Ser.* **1138**, 012003 (2018).
- [39] A. A. Schepetnov, D. A. Glazov, A. V. Volotka, V. M. Shabaev, I. I. Tupitsyn, and G. Plunien, *J. Phys. Conf. Ser.* **583**, 012001 (2015).
- [40] A. Wagner, S. Sturm, F. Köhler, D. A. Glazov, A. V. Volotka, G. Plunien, W. Quint, G. Werth, V. M. Shabaev, and K. Blaum, *Phys. Rev. Lett.* **110**, 033003 (2013).
- [41] V. A. Yerokhin and U. D. Jentschura, *Phys. Rev. A* **81**, 012502 (2010).
- [42] V. A. Yerokhin and Z. Harman, *Phys. Rev. A* **95**, 060501(R) (2017).
- [43] V. A. Yerokhin, C. H. Keitel, and Z. Harman, *J. Phys. B* **46**, 245002 (2013).
- [44] A. V. Volotka, D. A. Glazov, V. M. Shabaev, I. I. Tupitsyn, and G. Plunien, *Phys. Rev. Lett.* **103**, 033005 (2009).
- [45] A. V. Volotka, D. A. Glazov, V. M. Shabaev, I. I. Tupitsyn, and G. Plunien, *Phys. Rev. Lett.* **112**, 253004 (2014).
- [46] D. A. Glazov, A. V. Volotka, V. M. Shabaev, I. I. Tupitsyn, and G. Plunien, *Phys. Lett. A* **357**, 330 (2006).
- [47] D. A. Glazov, V. M. Shabaev, I. I. Tupitsyn, A. V. Volotka, V. A. Yerokhin, G. Plunien, and G. Soff, *Phys. Rev. A* **70**, 062104 (2004).
- [48] V. A. Yerokhin, A. N. Artemyev, and V. M. Shabaev, *Phys. Rev. A* **75**, 062501 (2007).
- [49] V. A. Yerokhin, *Phys. Rev. A* **83**, 012507 (2011).
- [50] R. A. Hegstrom, *Phys. Rev. A* **7**, 451 (1973).
- [51] G. Soff and P. J. Mohr, *Phys. Rev. A* **38**, 5066 (1988).
- [52] L. W. Fullerton and G. A. Rinker, *Phys. Rev. A* **13**, 1283 (1976).
- [53] S. Klarsfeld, *Phys. Lett. B* **66**, 86 (1977).
- [54] E. H. Wichmann and N. M. Kroll, *Phys. Rev.* **101**, 843 (1956).
- [55] F. Salvat and R. Mayol, *Comput. Phys. Commun.* **62**, 65 (1991).
- [56] F. Salvat, J. Fernández-Varea, and W. Williamson, *Comput. Phys. Commun.* **90**, 151 (1995).
- [57] A. G. Fainshtein, N. L. Manakov, and A. A. Nekipelov, *J. Phys. B* **24**, 559 (1991).
- [58] R. N. Lee, A. I. Milstein, I. S. Terekhov, and S. G. Karshenboim, *Can. J. Phys.* **85**, 541 (2007).
- [59] D. A. Glazov, A. V. Volotka, V. M. Shabaev, I. I. Tupitsyn, and G. Plunien, *Phys. Rev. A* **81**, 062112 (2010).
- [60] A. N. Artemyev, V. M. Shabaev, and V. A. Yerokhin, *Phys. Rev. A* **56**, 3529 (1997).
- [61] A. N. Artemyev, T. Beier, G. Plunien, V. M. Shabaev, G. Soff, and V. A. Yerokhin, *Phys. Rev. A* **60**, 45 (1999).
- [62] S. G. Karshenboim, V. G. Ivanov, and V. M. Shabaev, *J. Exp. Theor. Phys.* **93**, 477 (2001).
- [63] V. M. Shabaev, *Virial Relations for the Dirac Equation and Their Applications to Calculations of Hydrogen-Like Atoms*, in *Precision Physics of Simple Atomic Systems*, edited by S. G. Karshenboim and V. B. Smirnov (Springer, Berlin, Heidelberg, 2003), pp. 97–113.
- [64] M. E. Peskin and D. V. Schroeder, *An Introduction to Quantum Field Theory* (Westview Press, Boulder, 1995).
- [65] V. M. Shabaev, D. A. Glazov, A. V. Malyshev, and I. I. Tupitsyn, *Phys. Rev. A* **98**, 032512 (2018).

- [66] D. A. Glazov, A. V. Malyshev, V. M. Shabaev, and I. I. Tupitsyn, *Opt. Spectrosc.* **124**, 457 (2018).
- [67] I. A. Aleksandrov, D. A. Glazov, A. V. Malyshev, V. M. Shabaev, and I. I. Tupitsyn, *Phys. Rev. A* **98**, 062521 (2018).
- [68] D. A. Glazov, A. V. Malyshev, V. M. Shabaev, and I. I. Tupitsyn, *Phys. Rev. A* **101**, 012515 (2020).
- [69] H. Grotch and R. Kashuba, *Phys. Rev. A* **7**, 78 (1973).
- [70] P. J. Mohr, D. B. Newell, and B. N. Taylor, *Rev. Mod. Phys.* **88**, 035009 (2016).
- [71] F. Köhler, K. Blaum, M. Block, S. Chenmarev, S. Eliseev, D. A. Glazov, M. Goncharov, J. Hou, A. Kracke, D. A. Nesterenko, Y. N. Novikov, W. Quint, E. Minaya Ramirez, V. M. Shabaev, S. Sturm, A. V. Volotka, and G. Werth, *Nat. Commun.* **7**, 10246 (2016).
- [72] V. A. Yerokhin, K. Pachucki, M. Puchalski, Z. Harman, and C. H. Keitel, *Phys. Rev. A* **95**, 062511 (2017).
- [73] D. A. Glazov, F. Köhler-Langes, A. V. Volotka, K. Blaum, F. Heiße, G. Plunien, W. Quint, S. Rau, V. M. Shabaev, S. Sturm, and G. Werth, *Phys. Rev. Lett.* **123**, 173001 (2019).
- [74] J. P. Marques, P. Indelicato, F. Parente, J. M. Sampaio, and J. P. Santos, *Phys. Rev. A* **94**, 042504 (2016).
- [75] S. Verdebout, C. Nazé, P. Jönsson, P. Rynkun, M. Godefroid, and G. Gaigalas, *At. Data Nucl. Data Tables* **100**, 1111 (2014).
- [76] S. Sturm, I. Arapoglou, A. Egl, M. Höcker, S. Kraemer, T. Sailer, B. Tu, A. Weigel, R. Wolf, J. Crespo López-Urrutia, and K. Blaum, *Eur. Phys. J.: Spec. Top.* **227**, 1425 (2019).
- [77] R. Soria Orts, J. R. Crespo López-Urrutia, H. Bruhns, A. J. González Martínez, Z. Harman, U. D. Jentschura, C. H. Keitel, A. Lapiere, H. Tawara, I. I. Tupitsyn *et al.*, *Phys. Rev. A* **76**, 052501 (2007).